J Mater Sci: Mater Electron (2015) 26:8720–8725
DOI 10.1007/s10854-015-3548-4

Novel sol–gel method for synthesis of cobalt aluminate and its photocatalyst application

Saman Rahnamaeiyan[1] · Mahdi Nasiri[1] · Ruhollah Talebi[2] · Saeid Khademolhoseini[3]

Received: 20 June 2015 / Accepted: 27 July 2015 / Published online: 1 August 2015
© Springer Science+Business Media New York 2015

Abstract Pure cobalt aluminate ($CoAl_2O_4$) nanoparticles were successfully synthesized by novel sol–gel method with the aid of $Co(NO_3)_2{\cdot}3H_2O$, $Al(NO_3)_3{\cdot}9H_2O$, and gelatin without adding external surfactant or template. Besides, the effect of the dosage of gelatin on the particle size of final product was investigated. Moreover, gelatin plays role as capping agent, reducing agent, and chelate agent in the synthesis $CoAl_2O_4$ nanoparticles. The cobalt aluminate nanoparticles were characterized by using X-ray diffraction, scanning electron microscopy, ultraviolet–visible, Fourier transform infrared spectroscopy, and spectra energy dispersive analysis of X-ray techniques. To evaluate the catalytic properties of nanocrystalline cobalt aluminate, the photocatalytic degradation of methyl orange under visible light irradiation was carried out.

1 Introduction

In recent years, the preparation of low-dimensional nanostructures has been intensively pursued because of their useful applications in various areas. The sol gel method of preparing oxide powders generally involves polymerization via hydrolysis and condensation of an alkoxide, gelation, and heat treatment under suitable conditions [1–3]. Aluminum-based spinels constitute an interesting class of oxide ceramics with important technological applications. The impressive optical (e.g., $CoAl_2O_4$ is well known as Thenard's Blue) and chemical (catalytic applications) properties of transition-metal aluminates make them of significant interest as semiconductor and catalysts. For example spinel AMn_2O_4 (A=Cu, Zn) has been performed well for photocatalyzing water splitting into H_2 and O_2. Also, studies of aluminate system have focused on doping with the second activator, such as Nd, Eu and codoped with Er or Cr [4–6] that these studies are interesting. Transition metal aluminates are commonly prepared by a solid state reaction [7], coprecipitation method [8, 9], hydrothermal [10–12], combustion [13] and sol–gel [14–22]. The disadvantages of solid-state routes, such as inhomogeneity, lack of stoichiometry control, high temperature and low surface area, are improved when the material is synthesized using a solution-based method. Compared with other techniques, the sol–gel method is a useful and attractive technique for the preparation of aluminate spinels because of its advantage of producing pure and ultrafine powders at low temperatures. Transition metal-oxide spinels are important in many application fields because of their high thermal resistance and catalytic, electronic and optical properties. They are commonly used in semiconductor and sensor technology as well as in heterogeneous catalysis [23–27]. In this report, for the first time, we had presented the green approach for preparation of $CoAl_2O_4$ nanoparticles by novel sol–gel method in the presence of gelatin without adding external capping agent, capping agent or template. This approach is simple and friendly to the environment. The photocatalytic degradation was investigated using methyl orange (MO) under visible light irradiation ($\lambda > 400$ nm). The resulting degradation rates of the MO were measured to be as high as 90 % in 6 h.

✉ Mahdi Nasiri
nasiri.inline@gmail.com

[1] Young Researchers and Elite Club, Borujerd Branch, Islamic Azad University, Borujerd, Iran

[2] Young Researchers and Elite Club, Central Tehran Branch, Islamic Azad University, Tehran, Iran

[3] Young Researchers and Elite Club, South Tehran Branch, Islamic Azad University, Tehran, Iran

2 Experimental

2.1 Characterization

Cobalt nitrate hexahydrate ($Co(NO_3)_2{\cdot}6H_2O$), aluminium nitrate nonahydrate ($Al(NO_3)_3{\cdot}9H_2O$), were purchased from Merck Company and used without further purification. X-ray diffraction (XRD) patterns were recorded by a Philips-X'PertPro, X-ray diffractometer using Ni-filtered Cu Kα radiation at scan range of $10 < 2\theta < 80$. The electronic spectra of the cobalt aluminate were obtained on a Scinco UV–vis scanning spectrometer (Model S-10 4100). The energy dispersive spectrometry (EDS) analysis was studied by XL30, Philips microscope. Scanning electron microscopy (SEM) images were obtained on LEO-1455VP equipped with an energy dispersive X-ray spectroscopy. Fourier transform infrared (FT-IR) spectrum was recorded on a magna Nicolet 550 spectrophotometer in KBr pellets.

2.2 Synthesis of $CoAl_2O_4$ nanoparticles

In a typical synthesis, in two beakers separately, 2 and 1 mmol of $Co(NO_3)_2{\cdot}6H_2O$, $Al(NO_3)_3{\cdot}9H_2O$ were dissolved in 20 ml distilled water under stirring to form a homogeneous solution, respectively. Subsequently, different concentration of gelatin such as 0.5, 1, 2, and 4 g which are corresponding to the samples number 1–4, respectively were dissolved in 10 ml distilled water and was added to the $Co(NO_3)_2{\cdot}6H_2O$ solution under stirring at room temperature. Then, above solution was added to the $Al(NO_3)_3{\cdot}9H_2O$ solution. Afterwards, the final mixed solution was kept stirring to remove solvent and form a gel at 100 and 120 °C, respectively. Finally, the obtained product was calcinated at 800 °C for 135 min in a conventional furnace in air atmosphere. The synthesis conditions of $CoAl_2O_4$ nanoparticles are listed in Table 1.

2.3 Photocatalytic experimental

The MO photo degradation was examined as a model reaction to evaluate the photocatalytic activities of the $CoAl_2O_4$ nanoparticles. The photocatalytic experiments were performed under an irradiation wavelength of $\lambda > 400$ nm. The photo catalytic activity of nanocrystalline cobalt aluminate obtained from sample no. 4 was studied by the degradation of MO solution as a target pollutant. The photocatalytic degradation was performed with 0.001 g of MO solution containing 0.05 g of $CoAl_2O_4$. This mixture was aerated for 30 min to reach adsorption equilibrium. Later, the mixture was placed inside the photo reactor in which the vessel was 15 cm away from the visible source of 400 W Xeno lamp. The photo catalytic test was performed at room temperature. Aliquots of the mixture were taken at definite interval of times during the irradiation, and after centrifugation they were analyzed by a UV–vis spectrometer. The MO degradation percentage was calculated as:

$$\text{Degradation rate } (\%) = \frac{A0 - A}{A0} \times 100$$

where A0 and A are initial concentration and changed absorbencies of dye after visible light irradiation, respectively.

3 Results and discussion

The XRD pattern of pure $CoAl_2O_4$ nanoparticles (sample 4) is shown in Fig. 1. Extremely broaden reflection peaks were observed in Fig. 1, which indicated fine particle nature of the obtained cubic phase of $CoAl_2O_4$ nanoparticles. No other crystalline phases were detected in the calcined product. All the reflection peaks in this pattern could be readily indexed to the pure crystallite phase $CoAl_2O_4$ (JCPDS No. 44-0160), with the calculated cell parameters of $a = b = c = 8.1040$ Å. According to XRD data, the crystallite diameter (D_c) of $CoAl_2O_4$ nanoparticles obtained from sample 4 is calculated to be 40 nm using the Scherer Eq. (1) [28]:

$$D_c = K\lambda/\beta\cos\theta \qquad \text{Scherer equation}$$

where β is the breadth of the observed diffraction line at its half intensity maximum (400), K is the so-called shape factor, which usually takes a value of about 0.9, and λ is the wavelength of X-ray source used in XRD. To examine the effect of gelatin concentration on the morphology and particle size of final product four experiments were performed, as shown in Fig. 2a–d. According to the Fig. 2a, in the 0.5 gr concentration of gelatin, product mainly composed of inhomogeneous particles with average particle

Table 1 Reaction conditions for $CoAl_2O_4$ nanoparticles

Sample no.	Solvent	Gram gelatin	Temperature (°C)	Degradation MO
1	Water	0.5	800	–
2	Water	1	800	–
3	Water	2	800	–
4	Water	4	800	90 %

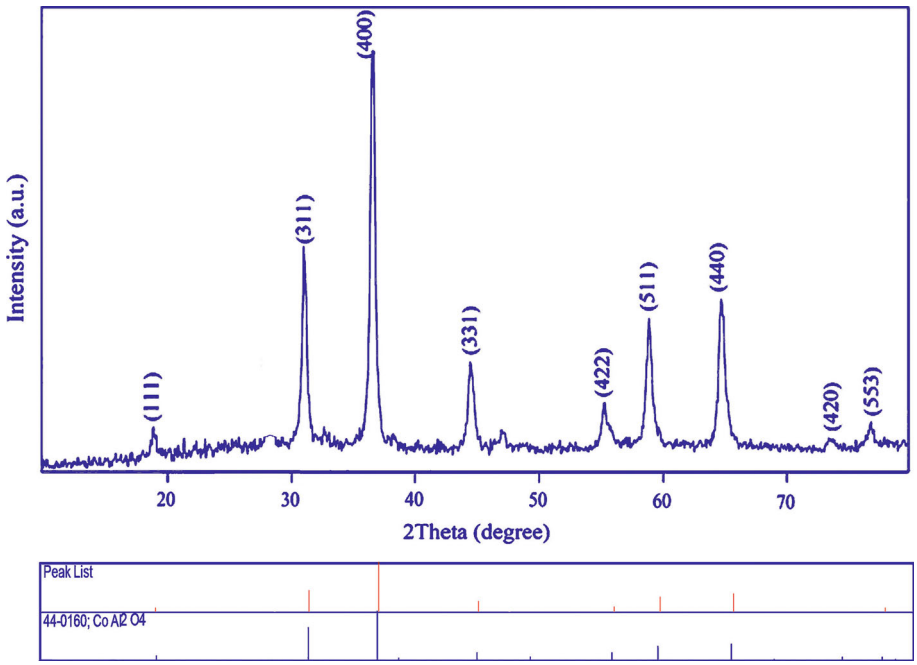

Fig. 1 XRD patterns of $CoAl_2O_4$ nanoparticles (sample no. 4)

size 60–80 nm. Increase in the concentration of gelatin from 0.5 to 1 gr, the particle size of the $CoAl_2O_4$ nanoparticles decreases (Fig. 2b). If we continued to increase the concentration of gelatin from 1 to 2 and 4 gr, the size and homogeneity of $CoAl_2O_4$ nanoparticles decrease and increase, respectively (Fig. 2c, d); therefore, optimum concentration of gelatin is 4 g. In order to examine the quality and chemical composition of the as-synthesized $CoAl_2O_4$ nanoparticles (sample 4), FTIR analysis was performed at room temperature in the range of 400–4000 cm^{-1} (Fig. 3). According to the Fig. 3, bands at 3432 and 1628 cm^{-1} are attributable to the v(OH) stretching and bending vibrations, respectively [29]. Furthermore, the metal–oxygen stretching frequencies are reported in the range 500–900 cm^{-1}, associated with the vibrations of M–O, Al–O, and M–O–Al bonds. Moreover, bands at 1119 and 1386 cm^{-1} are attributable to the C–O/C–C coupled stretching. EDS analysis was used to evaluate the chemical composition and purity of the as-synthesized $CoAl_2O_4$ nanoparticles (Fig. 3, sample 4). Based on the Fig. 4, Co, O, and Al elements are observed in the EDS spectrum. In addition, neither N nor C signals were detected in the EDS spectrum, which means the product is pure. The room temperature UV–vis absorption spectra of $CoAl_2O_4$ nanoparticles were also measured in the range of 200–600 nm. Figure 5a shows the diffuse reflection absorption spectra of the $CoAl_2O_4$ nanoparticles calcined at 800 °C. The figure indicates that the $CoAl_2O_4$ nanoparticles shows absorption maxima at 252 nm, the direct optical band gap estimated from the absorption spectra for the $CoAl_2O_4$ nanoparticles is shown in Fig. 5b. An optical band gap is obtained by plotting $(\alpha h\upsilon)^2$ versus $h\upsilon$ where α is the absorption coefficient and $h\upsilon$ is photon energy. Extrapolation of the linear portion at $(\alpha h\upsilon)^2 = 0$ gives the band gaps of 2.1 eV for $CoAl_2O_4$ nanoparticles. Photodegradation of MO under UV light irradiation (Fig. 6a–c) was employed to evaluate the photocatalytic activity of the as-synthesized $CoAl_2O_4$ (sample no. 4). No MO was practically broken down after 6 h without using Visible light irradiation or nanocrystalline $CoAl_2O_4$. This observation indicated that the contribution of self-degradation was insignificant. The probable mechanism of the photocatalytic degradation of MO can be summarized as follows:

$$CoAl_2O_4 + h\nu \rightarrow CoAl_2O_4^* + e^- + h^+ \quad (1)$$

$$h^+ + H_2O \rightarrow OH^{\cdot} \quad (2)$$

$$e^- + O_2 \rightarrow O_2^{\cdot -} \quad (3)$$

$$OH^{\cdot} + O_2^{\cdot -} + \text{methyl orange} \rightarrow \text{Degradation products} \quad (4)$$

Using photo catalytic calculations by Eq. (1), the MO degradation was about 90 % after 6 h irradiation of visible light, and nanocrystalline $CoAl_2O_4$ presented high photo catalytic activity (Fig. 6a). The spectrofluorimetric time-scans of MO solution illuminated at 510 nm with nanocrystalline $CoAl_2O_4$ are depicted in Fig. 6b shows continuous removal of MO on the $CoAl_2O_4$ under visible light irradiation. It is generally accepted that the heterogeneous photocatalytic processes comprise various steps

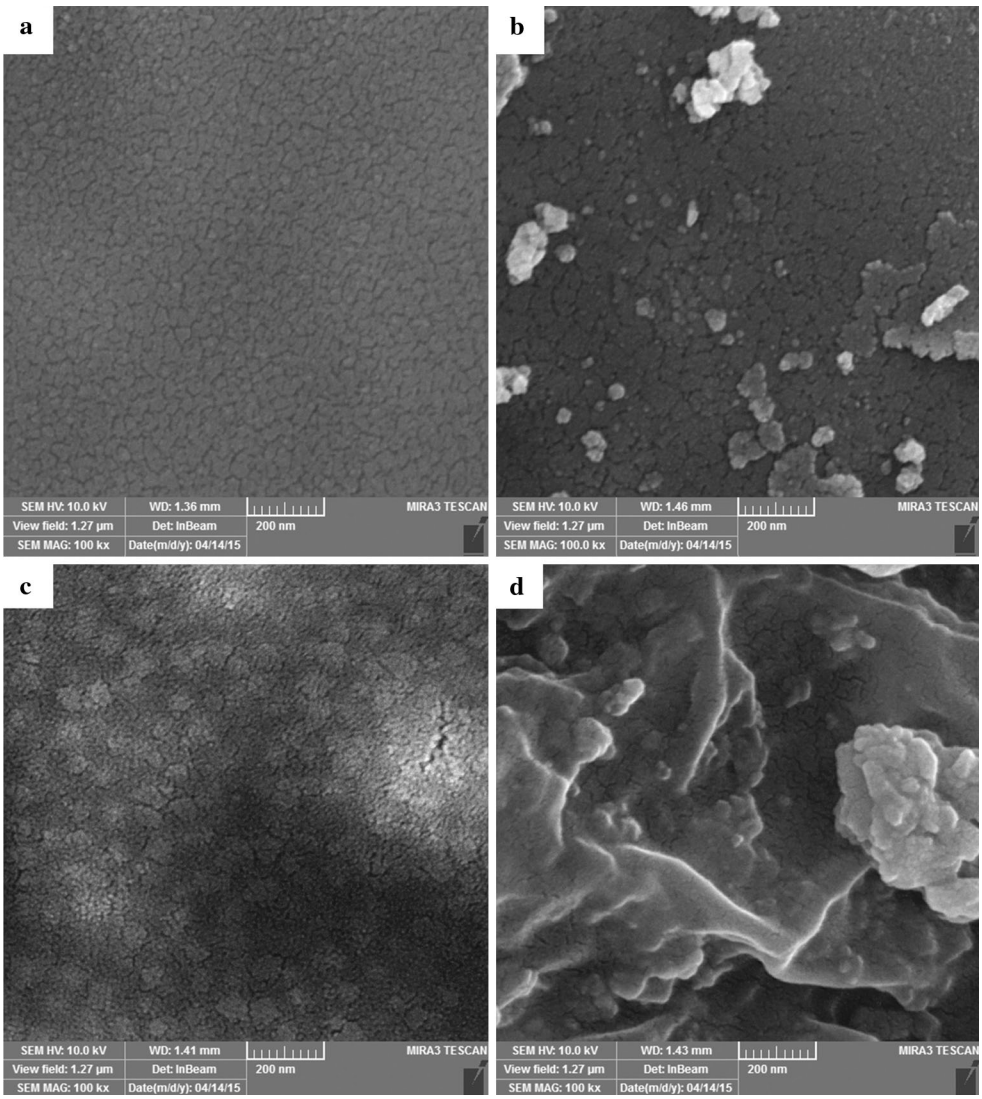

Fig. 2 SEM images of $CoAl_2O_4$ nanoparticles **a** sample no. 1 **b** sample no. 2 **c** sample no. 3 **d** sample no. 4

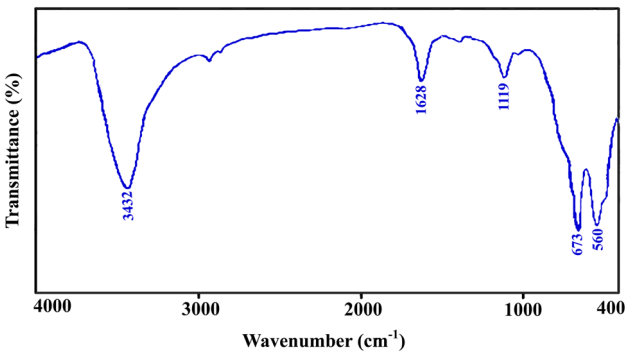

Fig. 3 FT-IR spectrum of $CoAl_2O_4$ nanoparticles (sample no. 4)

(diffusion, adsorption, reaction, and etc.), and suitable distribution of the pore in the catalyst surface is effective and useful to diffusion of reactants and products, which

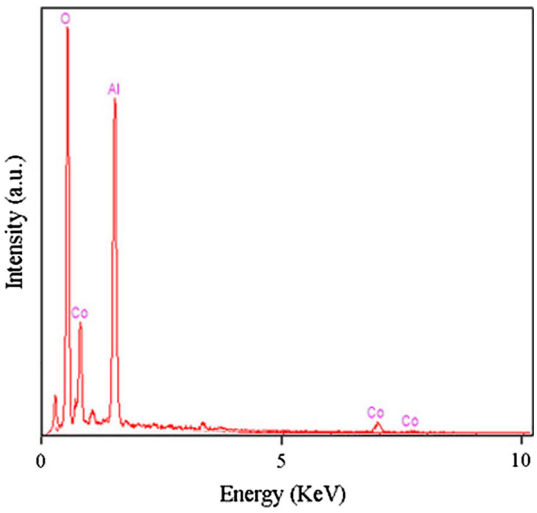

Fig. 4 EDS pattern of $CoAl_2O_4$ nanoparticles (sample no. 4)

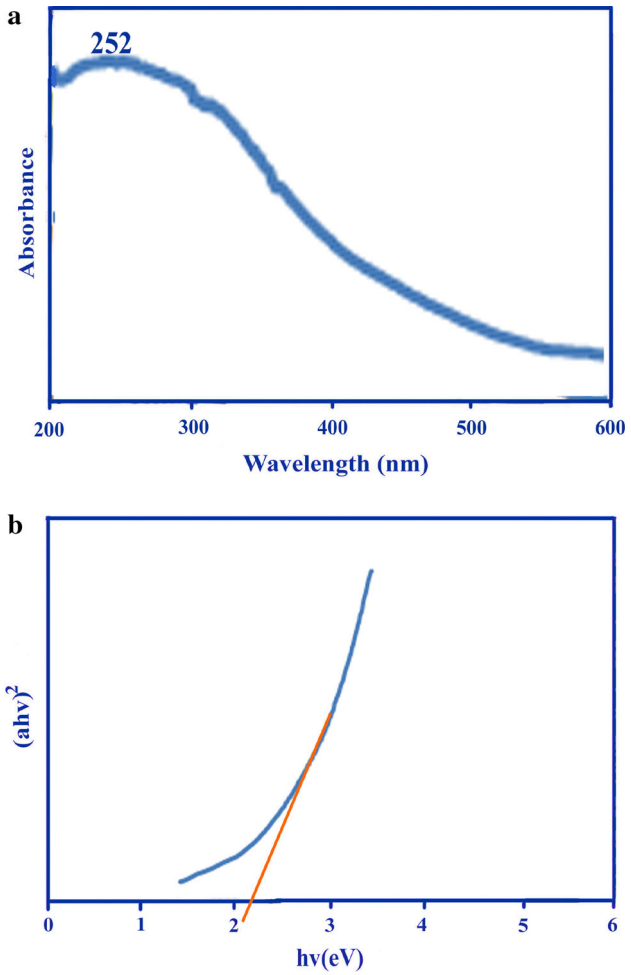

Fig. 5 Diffuse reflectance spectrum of $CoAl_2O_4$ nanoparticles (sample 4)

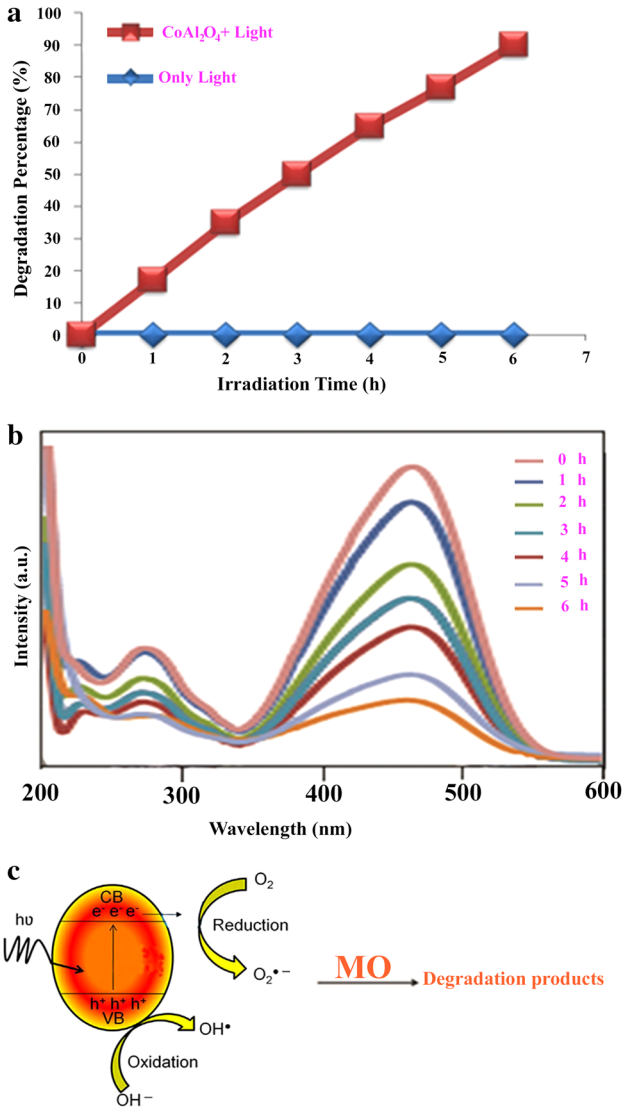

Fig. 6 Photocatalytic methyl orange degradation of $CoAl_2O_4$ nanoparticles obtained from sample no. 4 under visible light (**a**), fluorescence spectral time scan of methyl orange illuminated at 510 nm with $CoAl_2O_4$ nanoparticles (**b**), and reaction mechanism of methyl orange photodegradation over $CoAl_2O_4$ under visible light irradiation

prefer the photo catalytic reaction. In this investigation, the enhanced photocatalytic activity can be related to appropriate distribution of the pore in the nanocrystalline $CoAl_2O_4$ surface, high hydroxyl amount and high separation rate of charge carriers 24 (Fig. 6c).

4 Conclusion

$CoAl_2O_4$ nanoparticles were synthesized successfully via a novel sol–gel method in the presence of gelatin as reducing agent and Chelate agent. To investigate effect of gelatin concentration on the particle size of final product several experiments were performed. The products were analyzed by SEM, and ultraviolet–visible (UV–Vis) spectroscopy to be round, about 45–55 nm in size and Eg = 2.1 eV. When as-prepared nanocrystalline $CoAl_2O_4$ was utilized as photocatalyst, the percentage of MO degradation was about 90 % 6 h irradiation of visible light.

Acknowledgments Authors are grateful to council of University of Borujerd for providing financial support to undertake this work.

Compliance with ethical standards

Conflict of interest The author declares that the research was conducted in the absence of any commercial or financial relationships that could be construed as a potential conflict of interest.

References

1. F.M. Pontes, J.H.G. Rangel, E.R. Leite, E. Longo, J.A. Varela, E.B. Araú jo, J.A. Eiras, J. Mater. Sci. **36**, 3565 (2001)

2. O. Yamamoto, Y. Takeda, R. Kanno, M. Noda, Solid State Ion. **22**, 241 (1987)
3. H. Obayashi, Y. Sakurai, T. Gejo, J. Solid State Chem. **17**, 299 (1976)
4. Y. Shimizu, K. Uemura, N. Miura, N. Yamzoe, Chem. Lett. **67**, 1979 (1988)
5. T. Ivanova, A. Harizanova, M. Surtchev, Z. Nenova, Sol. Energy Mater. Sol. Cell. **76**, 591 (2003)
6. R. Sirera, M.L. Calzada, Mater. Res. Bull. **30**, 11 (1995)
7. D. Bersani, P.P. Lottici, A. Montenero, S. Pigoni, G. Gnappi, J. Non Cryst. Solids **490**, 192 (1995)
8. P.M.T. Cavalcante, M. Dondi, G. Guarini, M. Raimondo, G. Baldi, Dyes Pigm. **80**, 226 (2009)
9. L. Ji, S. Tang, H.C. Zeng, J. Lin, K.L. Tan, Appl. Catal. Gen. **207**, 2473 (2001)
10. Y. Bessekhound, M. Trari, Int. J. Hydrogen Energy **27**, 357 (2001)
11. X. Teng, W. Zhuang, Y. Hu, C. Zhao, H. He, X. Huang, J. Alloys Compd. **458**, 446 (2008)
12. H. Ryu, K.S. Bartwal, J. Alloys Compd. **464**, 317 (2008)
13. W.S. Hong, L.C. De Jonghe, X. Yang, M. Rahaman, J. Am. Ceram. Soc. **78**, 3217 (1995)
14. T. Mimani, J. Alloys Compd. **315**, 123 (2001)
15. M. Zawadzki, J. Wrzyszcz, Mater. Res. Bull. **35**, 109 (2009)
16. W.M. Shaheen, Thermochim. Acta **385**, 105 (2002)
17. Z. Chen, E. Shi, W. Li, Y. Zheng, N. Wu, W. Zhong, J. Am. Ceram. Soc. **85**, 2949 (2002)
18. A.K. Adak, A. Pathak, P. Pramanik, J. Mater. Sci. Lett. **17**, 559 (1998)
19. P. Thorma-hlen, E. Fridell, N. Cruise, M. Skoglundh, A. Palmqvist, Appl. Catal. B Environ. **31**, 1 (2001)
20. N.J. Van der Laag, M.D. Snel, P.C.M.M. Magusin, G. With, J. Eur. Ceram. Soc. **24**, 2417 (2004)
21. X.L. Duan, D.R. Yuan, X.Q. Wang, H.Y. Xu, J. Sol-Gel. Sci. Technol. **35**, 221 (2005)
22. X.L. Duan, D.R. Yuan, Z.H. Sun, C.N. Luan, D.Y. Pan, D. Xu, M.K. Lv, J. Alloys Compd. **386**, 311 (2005)
23. M. Salavati-Niasari, F. Davar, Z. Fereshteh, Chem. Eng. J. **146**, 498 (2009)
24. C.O. Arean, M.P. Mentruit, E.E. Platero, F.X.L. Xamena, J.B. Parra, Mater. Lett. **39**, 22 (1999)
25. W.S. Cho, M. Kahihana, J. Alloys Compd. **287**, 87 (1999)
26. C. Wang, S. Liu, L. Liu, X. Bai, Mater. Chem. Phys. **96**, 361 (2006)
27. A. Laobuthee, S. Wongkasemjit, E. Traversa, R.M. Laine, J. Eur. Ceram. Soc. **20**, 91 (2000)
28. M.Y. Li, W.S. Dong, C.L. Liu, Z. Liu, F.Q. Lin, J. Cryst. Growth **310**, 4628 (2008)
29. S. Ummartyotin, S. Sangngern, A. Kaewvilai, N. Koonsaeng, H. Manuspiya, A. Laobuthee, J. Sustain. Energy Environ. **1**, 31 (2009)